Electronic Supplementary Information

Superhydrophilic amorphous Co-B-P nanosheet electrocatalysts with Pt-like activity and durability for the hydrogen evolution reaction

Hongming Sun,[a] Xiaobin Xu,[b] Zhenhua Yan,[a] Xiang Chen,[a] Lifang Jiao,[a] Fangyi Cheng,*[a] Jun Chen [a,c]

[a.] Key Laboratory of Advanced Energy Materials Chemistry (Ministry of Education), College of Chemistry, Nankai University, Tianjin 300071. E-mail: fycheng@nankai.edu.cn.

[b.] Department of Chemistry and Biochemistry, University of California, Los Angeles, Los Angeles, CA 90095, USA.

[c.] State Key Laboratory of Elemento-Organic Chemistry, Innovative Collaboration Center of Chemical Science and Engineering, Nankai University, Tianjin 300071, China.

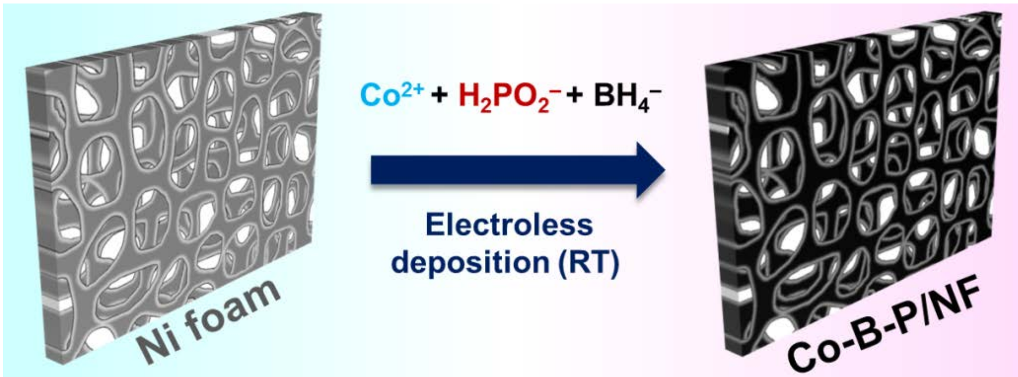

Fig. S1 Schematic illustration of the synthesis of Co-B-P supported on Ni foam.

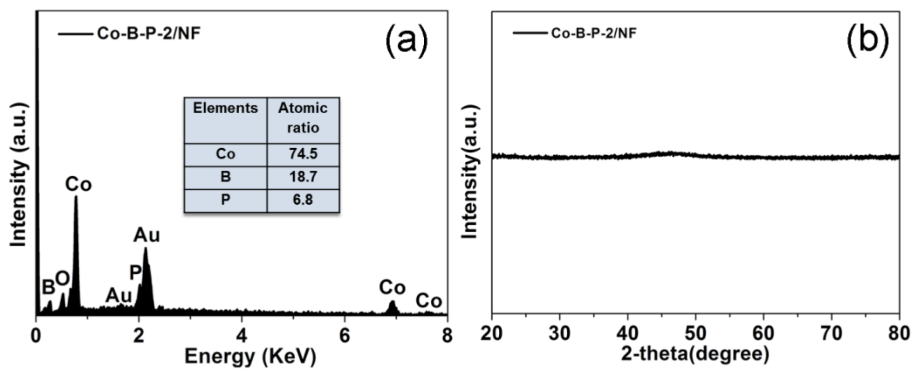

Elements	Atomic ratio
Co	74.5
B	18.7
P	6.8

Fig. S2 (a) EDS spectrum and elemental composition (inset) of Co-B-P-2/NF. (d) XRD pattern of Co-B-P-2/NF.

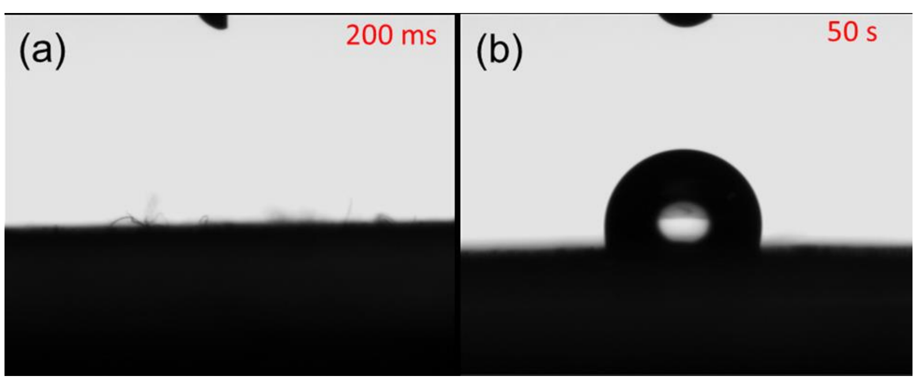

Fig. S3 The wettability test of Co-B-P nanosheet arrays (a) and Co-B-P nanospheres (b) deposited on Ni foil, respectively.

To eliminate the influence of the asperous substrate (Ni foam) for the contact angle measurements, the contact angles of Co-B-P nanosheet arrays and Co-B-P nanospheres loaded on Ni foil were also tested. The results indicate that Co-B-P nanosheet arrays on Ni foil is also hydrophilic, while contact angle between water and the Co-B-P nanospheres on Ni foil is measured to be 105.0°, showing non-hydrophilic (Video S1). The result is consistent with that of Co-B-P/NF and Co-B-P-2/NF (Fig. 1c,f insets).

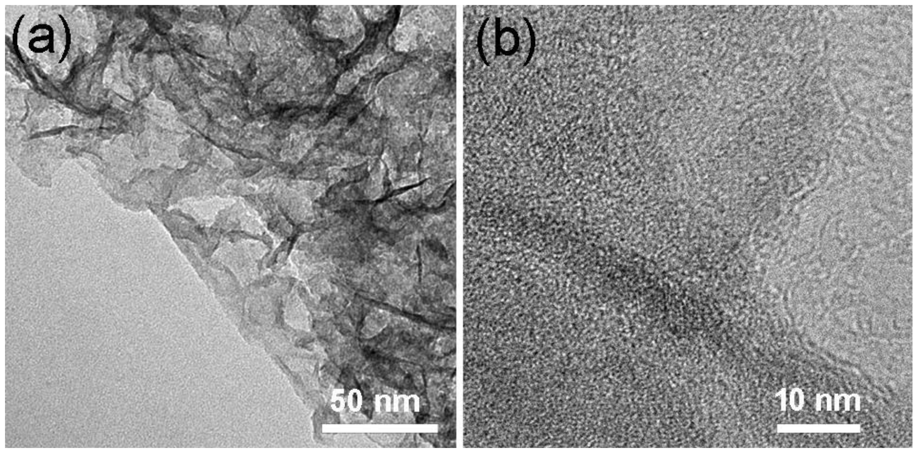

Fig. S4 (a, b) TEM images of Co-B-P/NF.

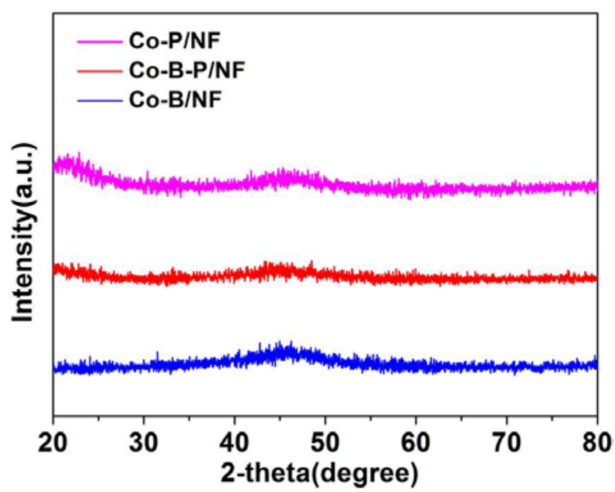

Fig. S5 XRD patterns of Co-P/NF, Co-B-P/NF and Co-B/NF.

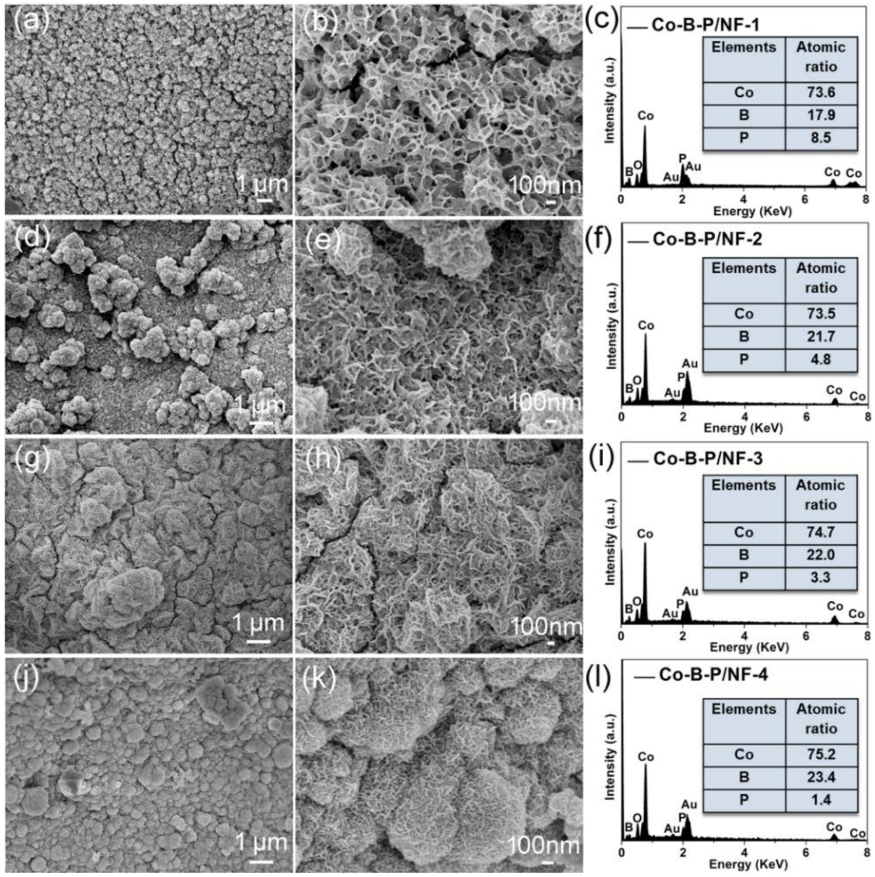

Fig.S6 SEM images, SEM-EDS spectroscopies and elemental composition analysis of (a-c) Co-B-P/NF-1, (d-f) Co-B-P/NF-2, (g-i) Co-B-P/NF-3, (j-l) Co-B-P/NF-4. The elemental compositions of Co-B-P/NF-1, Co-B-P/NF-2, Co-B-P/NF-3 and Co-B-P/NF-4 from EDS analysis were $Co_{2.80}B_{0.68}P_{0.32}$, $Co_{2.77}B_{0.82}P_{0.18}$, $Co_{2.95}B_{0.87}P_{0.13}$ and $Co_{3.03}B_{0.94}P_{0.06}$, respectively.

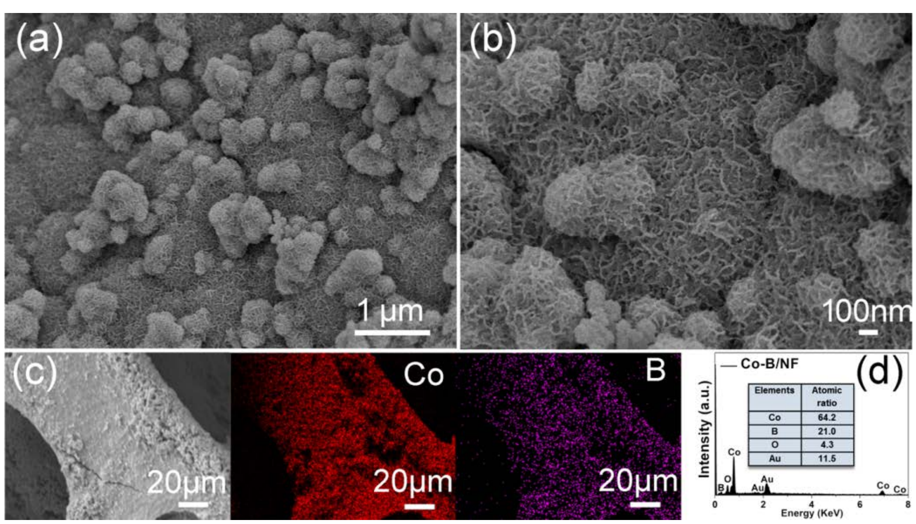

Fig. S7 (a) Low- and (b) high-magnification SEM images of Co-B/NF. (c) SEM image and EDS elemental mapping of Co and B. (d) The corresponding EDS spectrum and elemental composition analysis (inset).

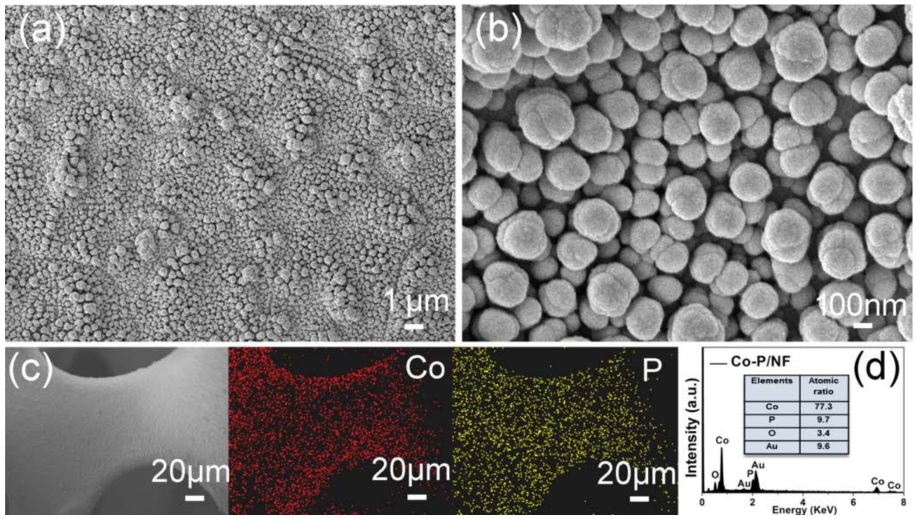

Fig. S8 (a) Low- and (b) high-magnification SEM images of Co-P/NF. (c) SEM image and elemental mapping of Co and P. (d) The corresponding EDS spectrum and elemental composition analysis (inset).

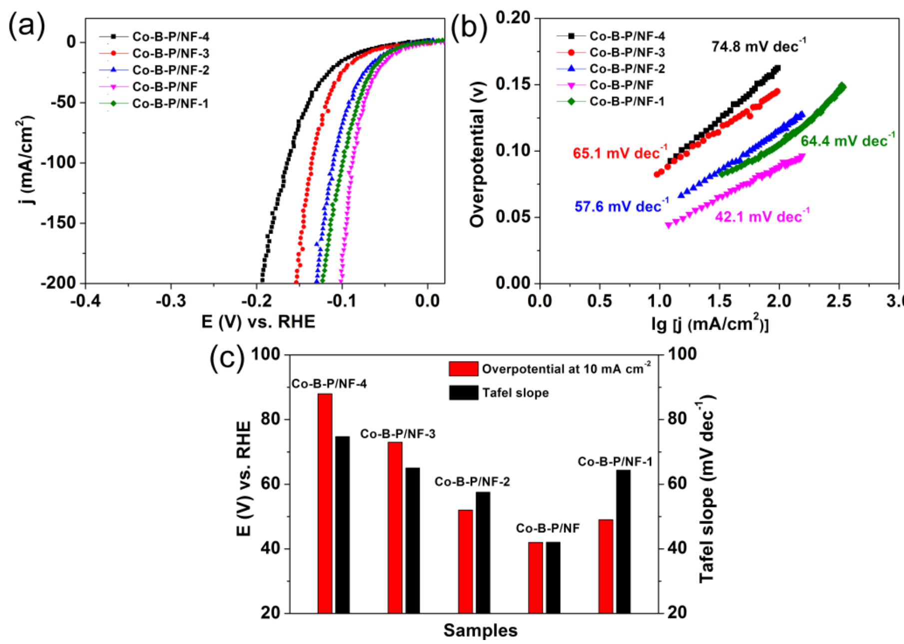

Fig.S9 (a) Polarization curves of Co-B-P/NF-1, Co-B-P/NF, Co-B-P/NF-2, Co-B-P/NF-3 and Co-B-P/NF-4 in 1 M KOH electrolyte. (b) Tafel plots derived from (a). (c) Comparison of the overpotentials at 10 mA cm^{-2} and Tafel slopes of the Co-B-P/NF-1, Co-B-P/NF, Co-B-P/NF-2, Co-B-P/NF-3 and Co-B-P/NF-4.

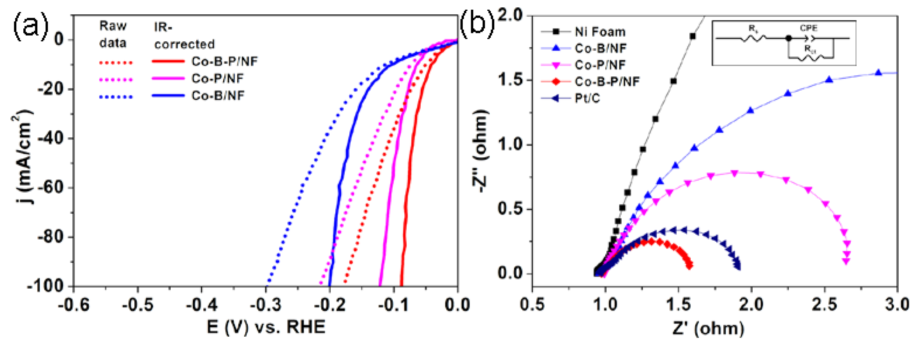

Fig. S10 (a) Original and iR-corrected polarization curves of Co-B-P/NF, Co-P/NF and Co-B/NF. (b) EIS Nyquist plots of Ni Foam, Co-B/NF, Co-P/NF, Co-B-P/NF and Pt/C recorded at overpotential of 100 mV.

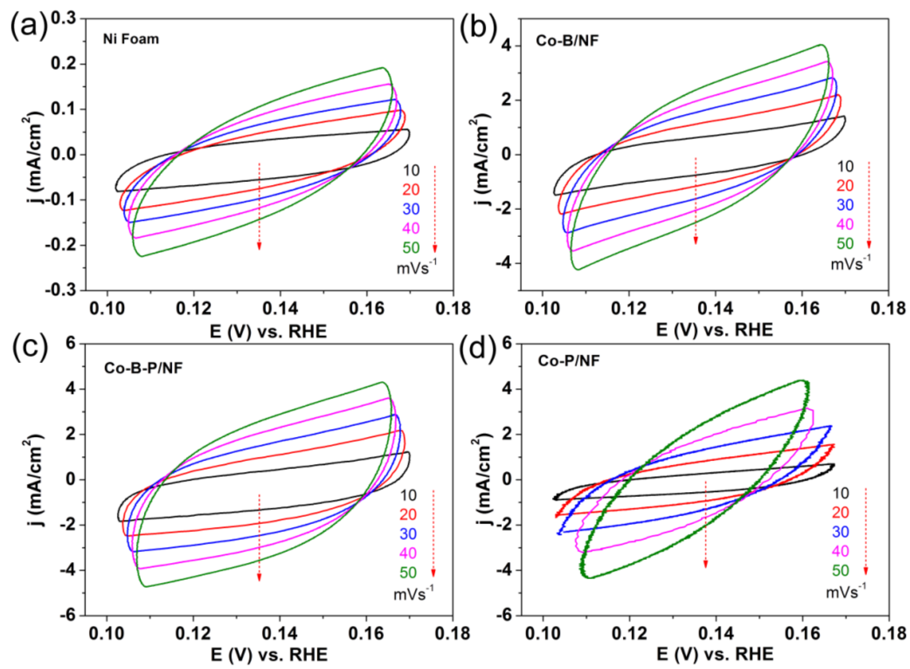

Fig. S11 CV curves recorded at different scan rates between 0.10 and 0.17 V for (a) Ni foam, (b) Co-B/NF, (c) Co-B-P/NF and (d) Co-P/NF.

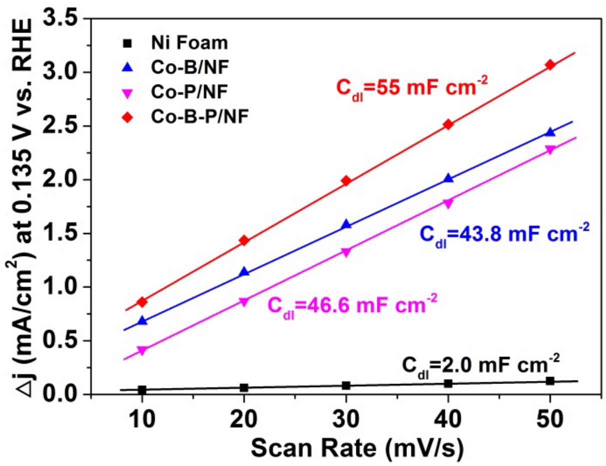

Fig. S12 Capacitive currents on the basis of scan rate for Ni foam, Co-B/NF, Co-P/NF and Co-B-P/NF at 0.135 V.

Calculation of electrochemically active surface area (ECSA):

The ECSA was determined assuming a C_{dl} capacitance (2 mF cm^{-2}) of Ni foam (Fig. S11), which was used as the substrate and considered as the reference.[s1]

$$A_{ECSA}^{Co\text{-}B/NF} = \frac{43.8\ \mathrm{mF\ cm^{-2}}}{2\ \mathrm{mF\ cm^{-2}\ per\ cm^2_{ECSA}}} = 21.9\ \mathrm{cm^2_{ECSA}}$$

$$A_{ECSA}^{Co\text{-}B\text{-}P/NF} = \frac{55\ \mathrm{mF\ cm^{-2}}}{2\ \mathrm{mF\ cm^{-2}\ per\ cm^2_{ECSA}}} = 27.5\ \mathrm{cm^2_{ECSA}}$$

$$A_{ECSA}^{Co\text{-}P/NF} = \frac{46.6\ \mathrm{mF\ cm^{-2}}}{2\ \mathrm{mF\ cm^{-2}\ per\ cm^2_{ECSA}}} = 23.3\ \mathrm{cm^2_{ECSA}}$$

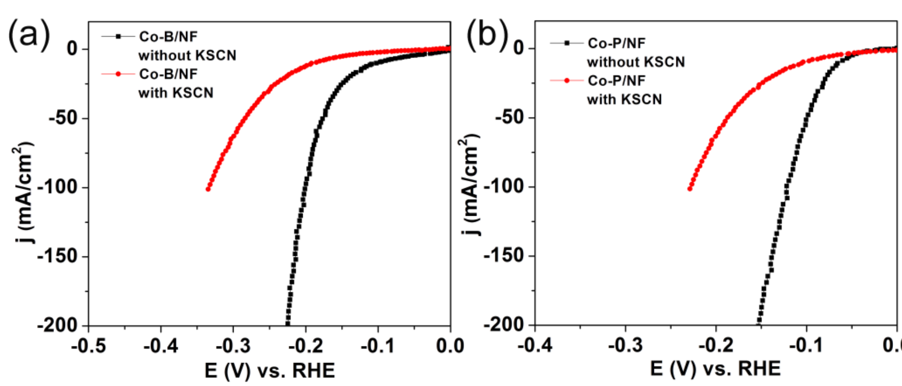

Fig. S13 (a) Polarization curves of Co-B/NF in 1 M KOH solution with or without 10 mM KSCN. (b) Polarization curves of Co-P/NF in 1 M KOH solution with or without 10 mM KSCN.

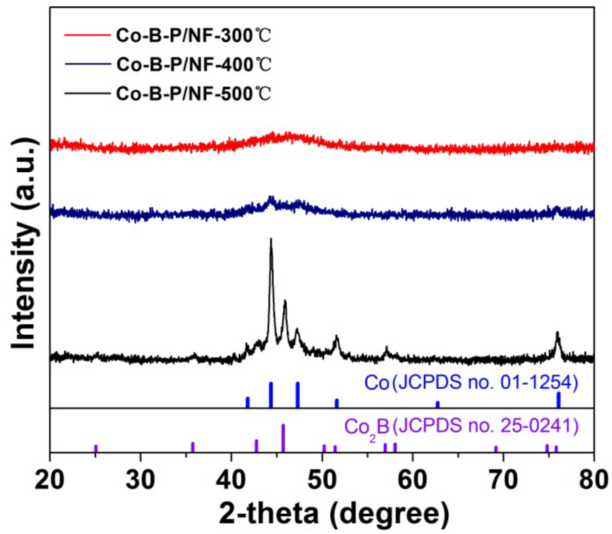

Fig.S14 The XRD patterns of Co-B-P/NF after thermal treatment at different temperatures for 2 h.

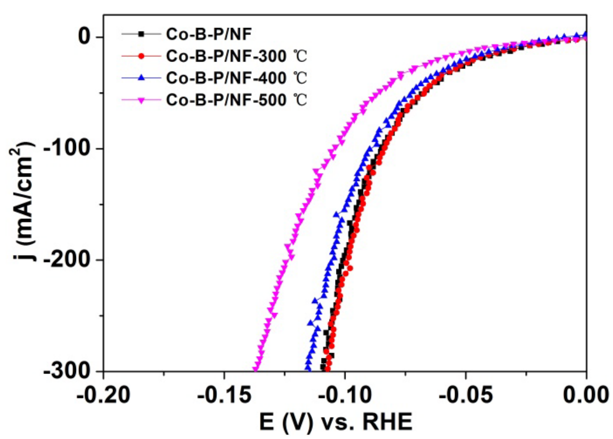

Fig. S15 The polarization curves of Co-B-P/NF after thermal treatment at different temperatures.

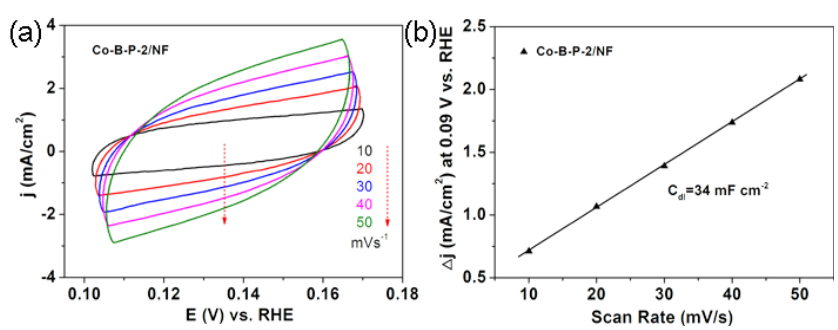

Fig. S16 (a) CV curves recorded at different scan rates between 0.10 and 0.17 V for Co-B-P-2/NF. (b) Capacitive currents on the basis of scan rate for Co-B-P-2/NF. Calculation of ECSA is given below:

$$A_{ECSA}^{Co\text{-}B\text{-}P\text{-}2/NF} = \frac{34\ \mathrm{mF\,cm^{-2}}}{2\ \mathrm{mF\,cm^{-2}}\ \text{per}\ \mathrm{cm_{ECSA}^2}} = 17.0\ \mathrm{cm_{ECSA}^2}$$

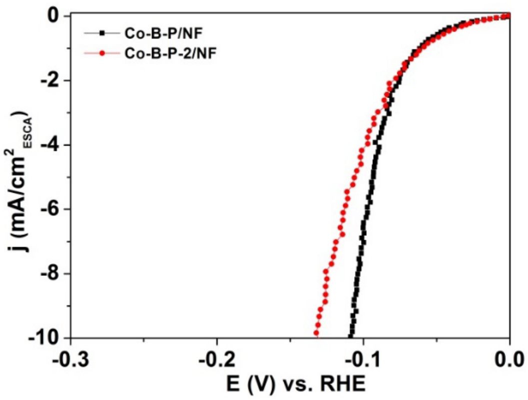

Fig. S17 ECSA-normalized initial polarization curves from Fig. 5a.

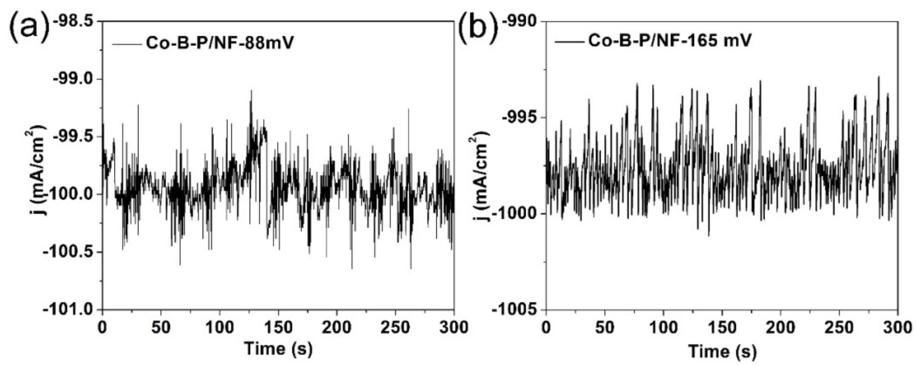

Fig. S18 Magnified chromoamperometry curves of Co-B-P/NF at overpotentials of 88 mV (a) and 165 mV (b).

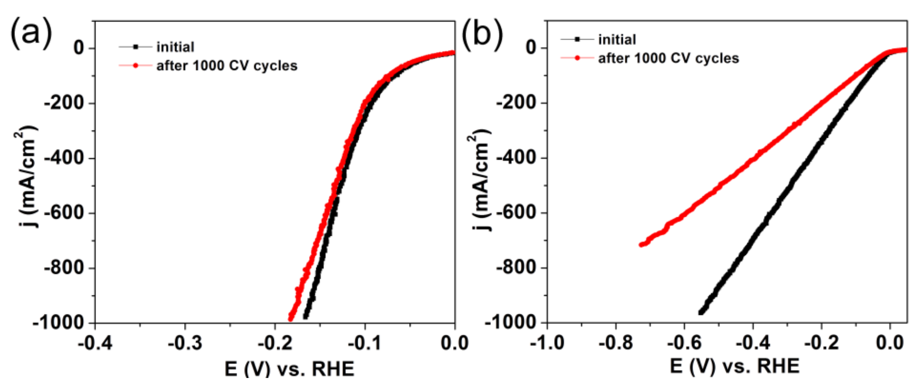

Fig. S19 Polarization curves of Co-B-P/NF (a) and Pt/C (b) in 1 M KOH before and after 1000 cycles at a scan rate of 100 mV s^{-1}.

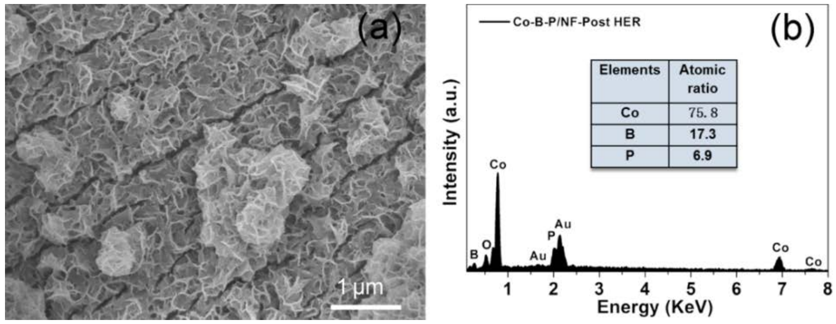

Fig. S20 (a) The SEM image and (b) EDS spectrum and elemental composition (inset) of Co-B-P/NF after the HER measurement at an overpotential of 88 mV for 20 h. The loading of Co-B-P on the Ni foam substrate before (5.12 mg cm^{-2}) and after (4.96 mg cm^{-2}) HER durability test was nearly maintained, indicating the good mechanical stability of the in-situ grown Co-B-P catalysts even at large working current density.

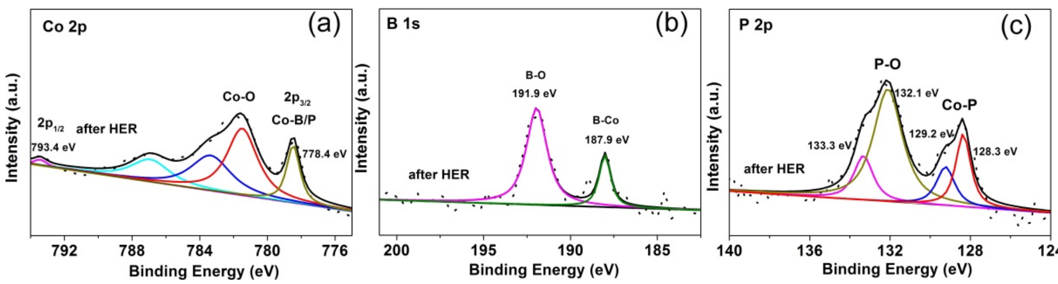

Fig. S21 High-resolution XPS spectra of (a) Co 2P, (b) B 1s and (c) P 2p after the HER measurement at an overpotential of 88 mV for 20 h.

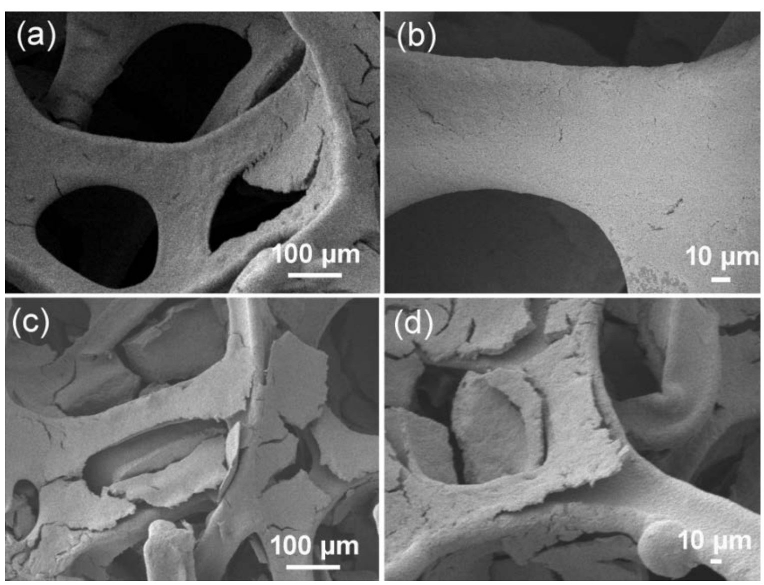

Fig. S22 The SEM images of Pt/C (20 wt%) loaded on Ni foam before (a,b) and after (c,d) the HER measurement.

Table S1. Comparison of the electrocatalytic HER activity of representative nonprecious HER catalysts in 1.0 M KOH electrolyte.

Catalyst	**Tafel slope (mV dec^{-1})**	**Overpotential (mV) at −10 mA cm^{-2}**	**Ref.**
Co-B-P/NF	**42.1**	**42**	**This work.**
Mo_2C@NC	…	60	S2
FeB_2	87.5	61	S3
Ni-Co-P Nanocubes	60.1	150	S4
Co-NRCNTs	…	370	S5
Co_9S_8/CC	83	150	S6
EG/H-$Co_{0.85}$Se|P	123.2	150	S7
NiCoP/rGO	124.1	209	S8
CoP_2/RGO	96	330	S9
Co/Co_3O_4	90	90	S10
Co_3O_4-MTA	98	…	S11
Co-B@CoO/Ti	78	102	S12
Co/CoP nanocrystals	66	135	S13
MoB	59	…	S14
$CoSe_2$/CF	52	95	S15
$Ni_{0.89}Co_{0.11}Se_2$ MNSN/NF	52	85	S16
NiO/Ni-CNT	51	…	S17
Ni-Mo/Ti	78	92	S18
$Co(S_{0.71}Se_{0.29})_2$	90	122	S19
Cu@CoS_x/CF	61	134	S20
MoS_2/Ni_3S_2	83.1	110	S21
O-Co_2P-3	61.1	160	S22
Ni-$B_{0.54}$	88	135	S23
Co@BCN	103.2	183	S24
rGO/$W_xMo_{1-x}S_2$	81.3	233	S25
Mo_2C@C	71	47	S26

Notes and references

s1. H. Liang, A. N. Gandi, D. H. Anjum, X. Wang, U. Schwingenschlögl and H. N. Alshareef, *Nano Lett.,* 2016, **16**, 7718−7725.
s2. Y. Liu, G. Yu, G. D. Li, Y. Sun, T. Asefa, W. Chen and X. Zou, *Angew. Chem., Int. Ed.,* 2015, **54**, 10752–10757.
s3. H. Li, P. Wen, Q. Li, C. Dun, J. Xing, C. Lu, S. Adhikari, L. Jiang, D. L. Carroll and S. M. Geyer, *Adv. Energy Mater.,* 2017, **7**, 1700513.
s4. Y. Feng, X. Yu and U. Paik, *Chem. Commun.,* 2016, **52**, 1633−1636.
s5. X. Zou, X. Huang, A. Goswami, R. Silva, B. R. Sathe, E. Mikmekova and T. Asefa, *Angew. Chem., Int. Ed.,* 2014, **53**, 4372–4376.
s6. L. L. Feng, M. Fan, Y. Wu, Y. Liu, G. D. Li, H. Chen, W. Chen, D. Wang and X. Zou, *J. Mater. Chem. A,* 2016, **4**, 6860–6867.
s7. Y. Hou, M. Qiu, T. Zhang, X. Zhuang, C. S. Kim, C. Yuan and X. Feng, *Adv. Mater.,* 2017, **2**, 1701589.
s8. J. Li, M. Yan, X. Zhou, Z. Q. Huang, Z. Xia, C. R. Chang, Y. Ma and Y. Qu, *Adv. Funct. Mater.,* 2016, **26**, 6785–6796.
s9. J. Wang, W. Yang and J. Liu, *J. Mater. Chem. A,* 2016, **4**, 4686–4690.
s10. X. Yan, L. Tian, M. He and X. Chen, *Nano Lett.,* 2015, **15**, 6015−6021.
s11. Y. P. Zhu, T. Y. Ma, M. Jaroniec and S. Z. Qiao, *Angew. Chem., Int. Ed.,* 2016, **55**, 1–6.
s12. W. Lu, T. Liu, L. Xie, C. Tang, D. Liu, S. Hao, F. Qu, G. Du, Y. Ma, A. M. Asiri and X. Sun, *Small,* 2017, **13**, 1700805.
s13. H. Wang, S. Min, Q. Wang, D. Li, G. Casillas, C. Ma, Y. Li, Z. Liu, L. Li, J. J. Yuan, M. Antonietti and T. Wu, *ACS Nano,* 2017, **11**, 4358–4364.
s14. H. Vrubel and X. Hu, *Angew. Chem.,Int. Ed.,* 2012, **51**, 12703–12706.
s15. C. Sun, Q. Dong, J. Yang, Z. Dai, J. Lin, P. Chen, W. Huang and X. Dong, *Nano Res.,* 2016, **9**, 2234–2243.
s16. B. Liu, Y. F. Zhao, H. Q. Peng, Z. Y. Zhang, C. K. Sit, M. F. Yuen, T. R. Zhang, C. S. Lee and W. J. Zhang, *Adv. Mater.,* 2017, **29**, 1606521.
s17. M. Gong, W. Zhou, M. C. Tsai, J. Zhou, M. Guan, M. C. Lin, B. Zhang, Y. Hu, D. Y. Wang, J. Yang, S. J. Pennycook, B. J. Hwang and H. Dai, *Nat. Commun.,* 2014, **5**, 4695.
s18. J. Tian, N. Cheng, Q. Liu, X. Sun, Y. He and A. M. Asiri, *J. Mater. Chem. A,* 2015, **3**, 20056–20059.
s19. L. Fang, W. Li, Y. Guan, Y. Feng, H. Zhang, S. Wang and Y. Wang, *Adv. Funct. Mater.,* 2017, **27**, 1701008.
s20. Y. Liu, Q. Li, R. Si, G. D. Li, W. Li, D. P. Liu, D. Wang, L. Sun, Y. Zhang and X. Zou, *Adv. Mater.,* 2017, **29**, 1606200.
s21. J. Zhang, T. Wang, D. Pohl, B. Rellinghaus, R. Dong, S. Liu, X. Zhuang and X. Feng, *Angew. Chem., Int. Ed.,* 2016, **55**, 1–7.
s22. K. Xu, H. Ding, M. Zhang, M. Chen, Z. Hao, L. Zhang, C. Wu and Y. Xie, *Adv. Mater.,* 2017, **29**, 1606980.
s23. P. Zhang, M. Wang, Y. Yang, T. Yao, H. Han and L. Sun, *Nano Energy,* 2016, **19**, 98–107.
s24. H. Zhang, Z. Ma, J. Duan, H. Liu, G. Liu, T. Wang, K. Chang, M. Li, L. Shi, X. Meng, K. Wu and J. Ye, *ACS Nano,* 2016, **10**, 684−694
s25. Y. Lei, S. Pakhira, K. Fujisawa, X. Wang, O. O. Iyiola, N. Perea Lopez, A. Laura Elias, L. Pulickal Rajukumar, C. Zhou, B. Kabius, N. Alem, M. Endo, R. Lv, J. L. Mendoza-Cortes and M. Terrones, *ACS Nano,* 2017, **11**, 5103–5112.
s26. Y. Y. Chen, Y. Zhang, W. J. Jiang, X. Zhang, Z. Dai, L. J. Wan and J. S. Hu, *ACS Nano,* 2016, **10**, 8851–8860.